2014 IEEE International Conference on Robotics & Automation (ICRA)
Hong Kong Convention and Exhibition Center
May 31 - June 7, 2014. Hong Kong, China

A Soft Wearable Robotic Device for Active Knee Motions using Flat Pneumatic Artificial Muscles

Yong-Lae Park[1], Jobim Santos[2], Kevin G. Galloway[2], Eugene C. Goldfield[2,3], and Robert J. Wood[2,4]

***Abstract*— We present the design of a soft wearable robotic device composed of elastomeric artificial muscle actuators and soft fabric sleeves, for active assistance of knee motions. A key feature of the device is the two-dimensional design of the elastomer muscles that not only allows the compactness of the device, but also significantly simplifies the manufacturing process. In addition, the fabric sleeves make the device lightweight and easily wearable. The elastomer muscles were characterized and demonstrated an initial contraction force of 38N and maximum contraction of 18mm with 104kPa input pressure, approximately. Four elastomer muscles were employed for assisted knee extension and flexion. The robotic device was tested on a 3D printed leg model with an articulated knee joint. Experiments were conducted to examine the relation between systematic change in air pressure and knee extension-flexion. The results showed maximum extension and flexion angles of 95° and 37°, respectively. However, these angles are highly dependent on underlying leg mechanics and positions. The device was also able to generate maximum extension and flexion forces of 3.5N and 7N, respectively.**

I. INTRODUCTION

Wearable robotic devices have increasingly gone beyond being laboratory curiosities to become an important tool for clinicians. A dominant design that has emerged from the laboratory is the exoskeleton with rigid frame structures [1]. Exoskeletons are often combined with high-torque electromechanical actuators for military applications [2], [3]. They are also considered as rehabilitation and/or assistive devices by employing lightweight, compliant (or elastic) actuators [4], [5], [6].

While there are certain advantages that are derived from traditional exoskeleton design, such as relatively transparent force transmission and rigid mechanical body supports, they also carry several practical limitations, including bulkiness, mechanical constraints to host bodies, and safety issues when the wearers physically interact with other people. A new design, soft exoskeletons, overcome such limitations by removing rigid frame structures and mechanical joints. Such systems include active soft orthotic devices for assistance of ankle [7], [8] and knee [9], [10] motions, a compliant exo-suit for improved metabolic energy efficiency through active gait assistance [11], and upper extremity rehabilitation with cable-driven [12] and pneumatic muscle [13] actuations. The design of soft exoskeletons is guided by the biomechanical properties of the human body so that synthetic components harness the elastic properties of soft tissue and the mechanical advantage of the skeletal levers. However, currently available actuation mechanisms limit further miniaturization and weight reduction of the devices, resulting in reduced wearability.

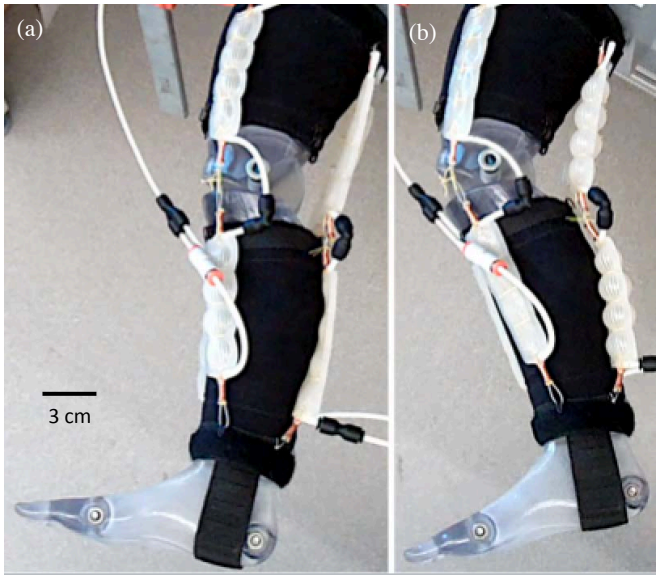

Fig. 1. A Second Skin prototype in action. (a) Active knee extension. (b) Active knee flexion.

Therefore, further progress in this emerging field will depend on a new class of soft active materials for mechanical actuation, and controllable compliance. Devices constructed from these materials are intended to be worn around wrist or knee joints and assist in the motor tasks of patients with neuromuscular injury or with limited motor control. When active, these devices should be capable of exerting assistive forces through dramatic but reversible changes in shape and elastic rigidity. While passive, such devices should not constrain the natural degrees of freedom of the host joints.

In this paper, we describe the design and characterization

*This work was supported by the Wyss Institute for Biologically Inspired Engineering and National Science Foundation (NSF) grant CNS 0932015. Any opinions, figures, and conclusions or recommendations expressed in this material are those of the authors and do not necessarily reflect the views of the NSF.

[1]Yong-Lae Park is with the Robotics Institute and the School of Computer Science, Carnegie Mellon University, Pittsburgh, PA 15213, USA (E-mail: ylpark@cs.cmu.edu).

[2]Jobim Santos, Kevin G. Galloway, Eugene C. Goldfield, and Robert J. Wood are with the Wyss Institute for Biologically Inspired Engineering, Harvard University, Boston, MA 02115, USA (E-mails: jobim.santos@wyss.harvard.edu; kevin.galloway@wyss.harvard.edu; eugene.goldfield@childrens.harvard.edu; rjwood@eecs.harvard.edu).

[3]Eugene C. Goldfield is also with the Boston Children's Hospital, Boston, MA 02155, USA.

[4]Robert J. Wood is also with the School of Engineering and Applied Sciences (SEAS), Harvard University, Cambridge, MA 02138, USA.

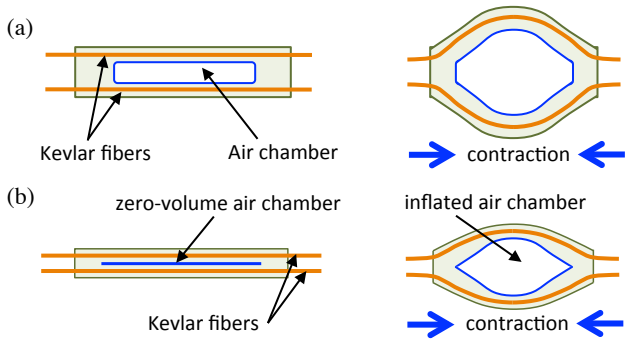

Fig. 2. Comparison of air chamber designs. (a) Conventional air chamber. (b) Zero-volume air chamber with reduced thickness.

of a soft wearable robotic assistive device (Fig. 1) for rehabilitation of injured nervous systems, called the "Second Skin." The device is composed of pneumatic elastomer actuators and fabric sleeves. A key feature of the device is the two-dimensional design of the elastomer muscles that not only allows the compactness of the device, but also significantly simplifies the manufacturing process. In addition, fabric sleeves make the device easily wearable and lightweight.

The remainder of the paper is organized as follows: an overview of the design and the fabrication of the actuator and the Second Skin device is described in Sec. II; a discussion of the characterization results is given in Sec. III; current research challenges and conclusions are discussed in Sec. IV and Sec. V, respectively.

II. DESIGN

A. Flat Pneumatic Artificial Muscle Design and Fabrication

We developed a simplified version of pneumatic artificial muscles that has a two-dimensional flat configuration. By remaining flat in its relaxed state, this version of the muscle is highly compact, adding little additional volume to host body when worn as a suit. The flat configuration our muscles not only provides a compact form factor suitable for a device worn on the skin surface, but also makes it possible to resize and reconfigure each individual muscle array. Furthermore, we introduced a new concept of zero-volume air chamber to further reduce the thickness of the muscles. In conventional design, such as traditional McKibben muscles [14], straight-fiber embedded rubber muscles [15], and pleated pneumatic muscles [16], a certain volume of an air chamber must exist in the structure although it is not actuated. However, our new concept of zero-volume air chamber completely removes this useless empty volume and makes the structure compact, as illustrated in Fig. 2. Furthermore, this 2-D configuration significantly simplifies the manufacturing process. The embedded straight Kevlar fibers[1] (diameter: 350 μm), which are flexible but inextensible, constrain the circumference of the air chamber and consequently creates horizontal contraction force and displacement when the air chamber is pressurized.

[1]8800K41, McMaster-Carr.

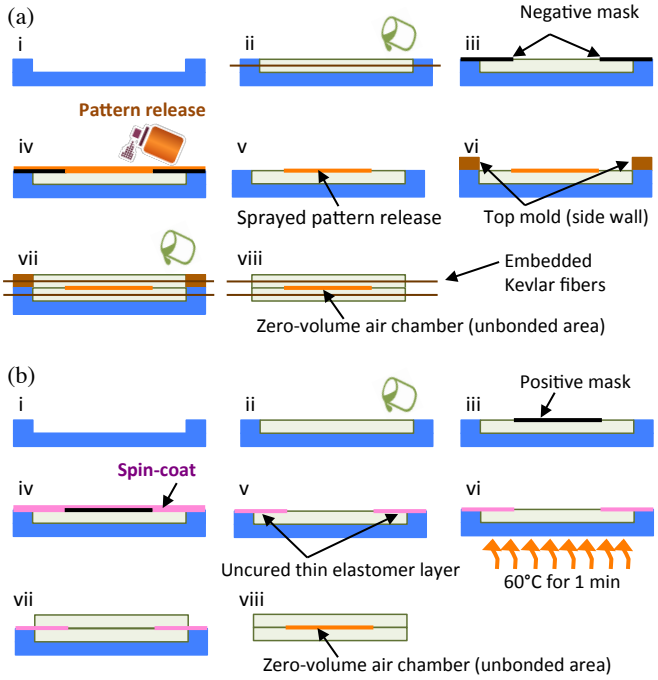

Fig. 3. (a) Fabrication process for a flat pneumatic artificial muscle actuator with a zero-volume air chamber using a negative mask and pattern release (i: Prepare a bottom mold, ii: Pour liquid elastomer for a bottom layer and embed Kevlar fibers, iii: Place a negative mask, iv: Spray pattern release, v: Remove the mask, vi: Place a top mold, vii: Pour liquid elastomer for a top layer and embed Kevlar fibers, and viii: Remove the top and bottom molds when the elastomer cures.). (b) Alternative fabrication process to make a zero-volume air chamber using a positive mask and spin-coating (i: Prepare a bottom mold, ii: Pour liquid elastomer for a bottom layer, iii: Place a positive mask, iv: Spin coat liquid elastomer, v: Remove the mask, vi: Partial bake, vii: Laminate a cured top layer, and viii: Remove the top and bottom molds when the elastomer layers bond with cure.).

The base material of the air chamber is highly stretchable silicone rubber[2]

Two slightly different fabrication processes for a zero-volume air chamber are illustrated in Fig. 3. Fig. 3-a uses pattern release sprayed on the unmasked area to prevent the bottom layer from becoming bonded to the top layer. However, Fig. 3-b, as an alternative method, uses a positive mask placed on the top surface of the cured bottom layer for preventing liquid elastomer from being coated. The latter method requires a bonding process of two cured layers while the former method repeats pouring processes to build a structure. This process makes a single unit zero-volume air chamber. By connecting multiple muscle cells in series, a multi-cell muscle can be made. While a serial configuration of multiple muscle cells increases the contraction length, a parallel configuration may increase the contraction force.

Fig. 4 shows an actual prototype of a flat pneumatic artificial muscle and its behavior. The size of the muscle is 80mm x 20mm x 3.5mm, and each muscle includes four muscle cells (zero-volume air chambers). The size of each cell is 8mm x 14 mm. This four cell muscle was employed to build our Second Skin prototype. The weight of

[2]Dragon Skin 10, Smooth-On Inc.

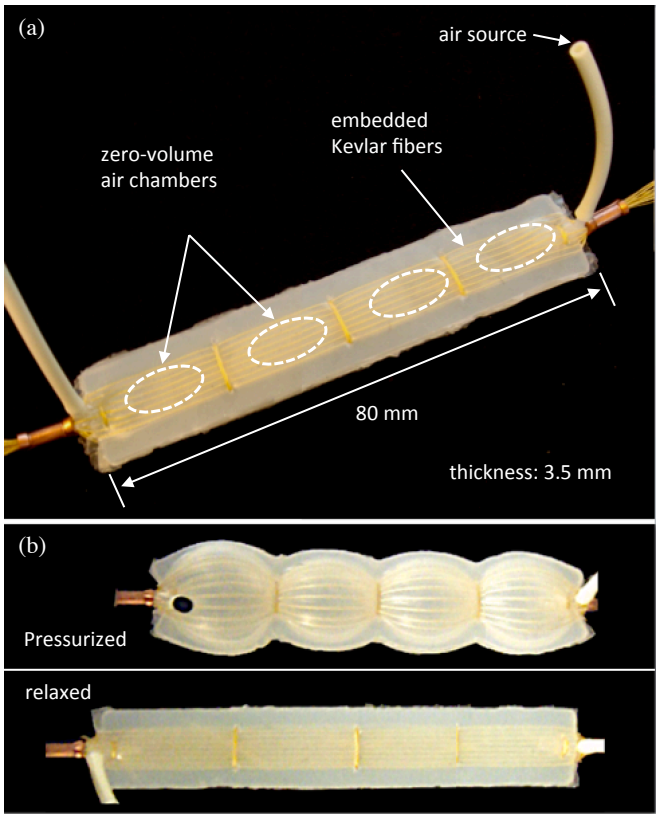

Fig. 4. A complete flat pneumatic artificial muscle prototype. (a) Four cell (air chamber) artificial muscle. (b) Contraction behavior with input pressure.

a single muscle, including tubing and attachment features, is approximately 8.4g.

B. Second Skin Prototyping

The overall structure of the device is a two-piece stretchable fabric sleeve with artificial muscles part of the outermost layer. By incorporating an array of the muscles with a form-fitting sleeve, a wearable assistive device was built, as shown in Fig. 5. The sleeve was tested on a 3D-printed leg model with an articulated knee joint (Fig. 5-a). This model was scaled to approximate a 50th percentile 12-month-old infant's leg based on [17], [18], since we are aiming to use our device for infant-toddler rehabilitation. The weights of the leg model and the sleeves are approximately 388g (thigh: 188g, ower leg: 200g) and 35g (thigh sleeve: 16g, lower leg sleeve: 19g), respectively. The actuators are connected to hooks at the ankle, the knee, or the top of the thigh (Fig. 5-b). Once the actuators are installed, the hook areas of the device are wrapped around with non-stretchable nylon straps. These nylon straps not only prevent the hook areas from being deformed by the pulling forces of the actuators, but also reduce the slip effect of the fabric on the wearer's skin. Multiple actuators may be arranged in parallel and/or series for increased contraction force and/or length, respectively. To maximize the angular displacement of the knee, actuators are connected from the ankle to the top of the thigh. To maximize the force of bending, actuators are connected from the ankle

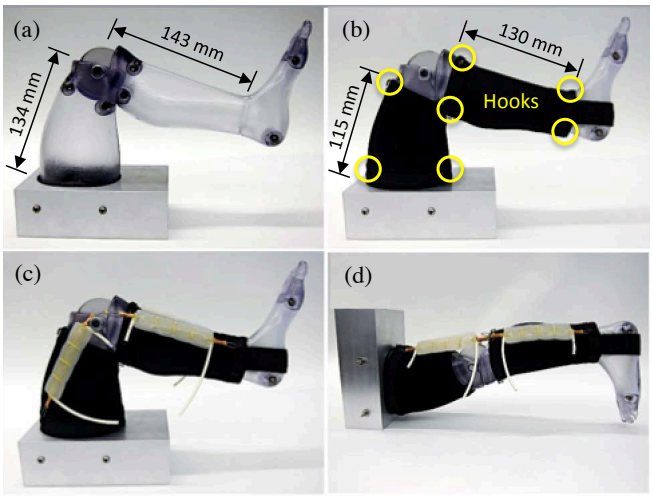

Fig. 5. Second Skin prototype structures. (a) A 3D printed leg model. (b) Stretchable fabric sleeves with multiple hooks. (c) Anterior muscle installation. (d) Posterior muscle installation.

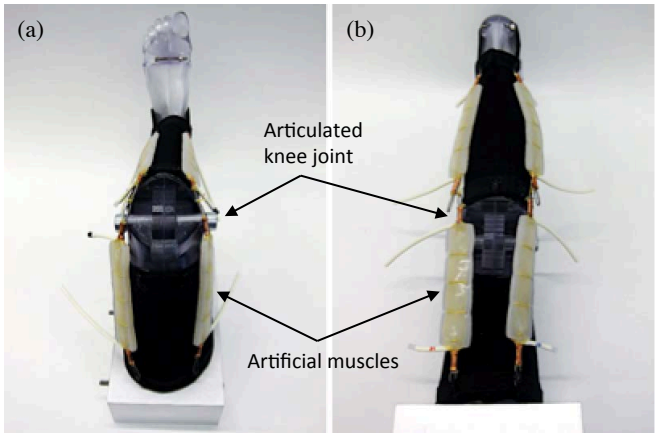

Fig. 6. A complete Second Skin prototype with artificial muscle installation. (a) Anterior side. (b) Posterior side.

to the top of the knee and from the top of the thigh to the bottom of the knee. A complete prototype with total eight muscles is shown in Fig. 6.

With two pairs of two muscles connected in series on the anterior side of the leg between the ankle and the top of the thigh (total four muscles), the device is able to fully extend the lower leg from less than a 90° knee angle (Fig. 7-a). With the same actuator arrangement on the posterior side of the leg, the device is able to flex the lower leg up to a 37° knee angle approximately from a fully extended knee position (Fig. 7-b).

III. RESULTS

A. Flat Pneumatic Artificial Muscle Characterization

We first characterized individual muscles using our custom-built test setup, shown in Fig. 8. We installed a commercial single-axis load cell[3] with an accuracy of 0.02%

[3]STL-50, AmCells Corp.

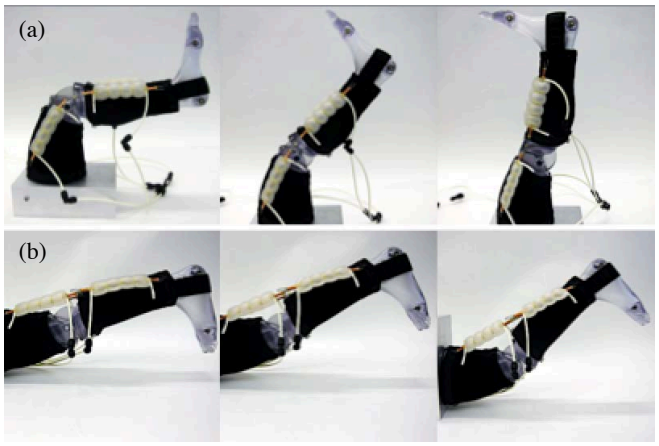

Fig. 7. Possible actuation motions of Second Skin prototype. (a) Active knee extension using anterior artificial muscles. (b) Active knee flexion using posterior artificial muscles.

for measuring contraction force of the muscle in a rigid frame. Using a hand crank, we were able to manually apply different tensions to the muscle and measure its extension and contraction lengths. The air pressure to the muscle is controlled by a pressure regulator. The load cell's voltage output is measured using a precision multi-meter and converted to a force value.

For characterization, a single muscle was installed in the test frame and pressurized with a constant air pressure with no axial displacement allowed. Then, the muscle was gradually released using a hand crank until the contraction force measured by the load cell becomes zero. During this release, the force profile was recorded. By repeating this process with different air pressures, the full characterization plot can be prepared, as shown in Fig. 9. The characterization result shows that the muscle is able to generate the maximum initial force of approximately 38N and create the contraction displacement up to approximately 18mm with 104kPa air pressure.

B. Second Skin Characterization

The angular displacement of the lower leg was measured using a manual goniometer as the air pressure of the muscles varied for both extension and flexion motions. In order to understand the behavior of the combined leg-device system, it was necessary to consider the anatomy and mechanical properties of the biological leg. Since we are aiming to use our device for rehabilitation of infants or early toddlers, who still spend most of their time lying either on the back or on the belly, we decided to test our device in the similar positions. Fig. 10 shows the results of these characterization tests when the lower leg is actuated from the fully flexed and extended positions. In each case, the lower leg was either extended or flexed with actuation and released back to the original position using gravity.

In the active leg extension test, a large hysteresis was observed between the two angle-pressure curves (Fig. 10-a). This is due to the initial position of the lower leg. In the rest

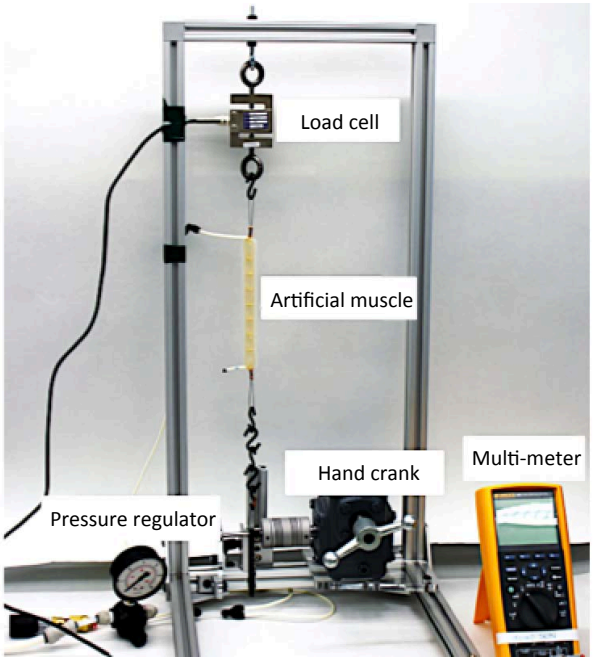

Fig. 8. Experimental setup for single muscle characterization.

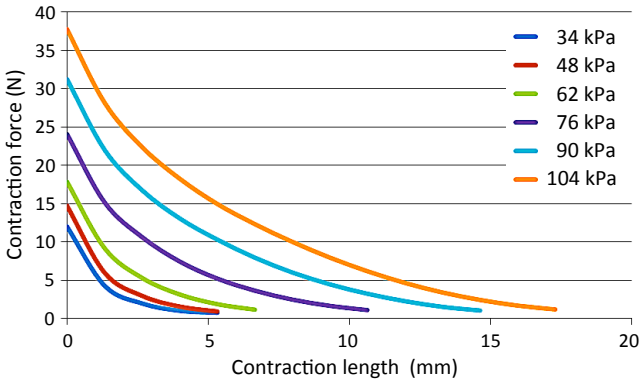

Fig. 9. Actuation characterization result of flat pneumatic artificial muscle

position, the distance between the axis of rotation and the lower leg's center of mass becomes almost the maximum, which requires high torque to overcome gravity for lifting up the lower leg. However, as the lower leg is raised, the center of mass rapidly moves toward the axis of rotation, which, in consequence, significantly reduces the reaction torque due to gravity. Once the leg reaches a certain point, it becomes fully extended and the actuators come fully aligned. It remains aligned until the actuator pressure decreases by a significant amount (approximately 30% in this test). The maximum extension angle achieved by actuation in this test was approximately 95°.

The hysteresis was significantly reduced in the active flexion test (Fig. 10-b). This is due to the much smaller maximum knee bending angle than that of of active extension. During flexion, the muscles always stay aligned to a straight line and its distance from the axis of rotation gradually

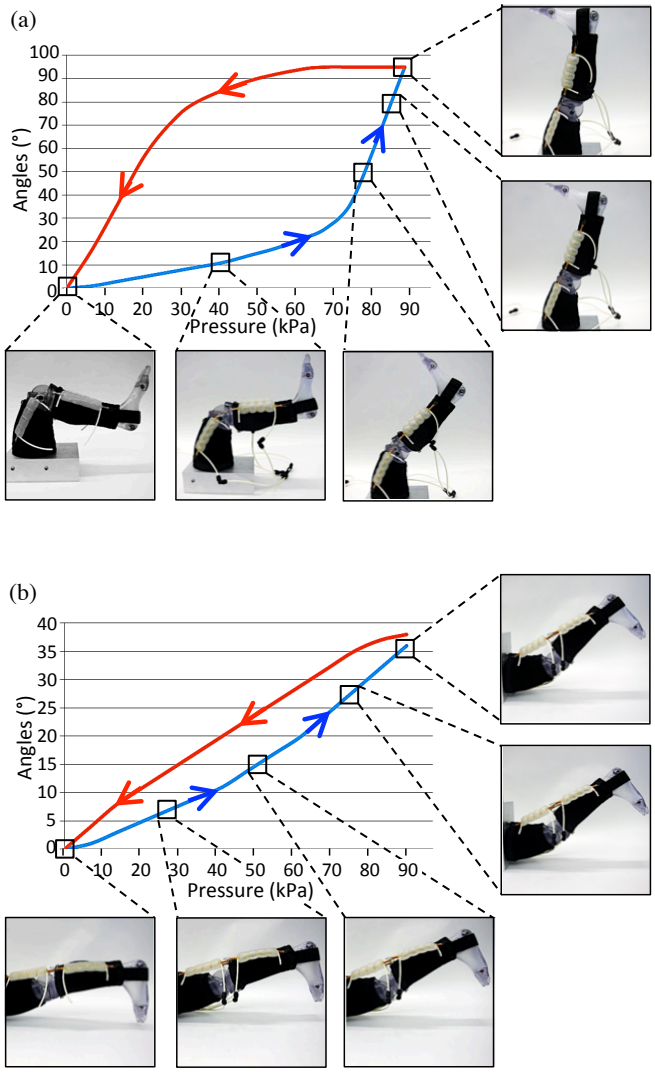

Fig. 10. Experimental results of active angular displacement characterization. (a) Knee extension result. (b) Knee flexion result.

increases. Although this may increase the torque applied to the knee joint, it simultaneously decreases the angular displacement. This linear response can be also observed in the previous extension test up until approximately 30° knee angle. The maximum flexion angle achieved by actuation in this test was approximately 37°.

In both tests, the device showed high repeatability, with only 1°-3° knee angle variations with several iterations. These variations were mostly caused by slip of the device on the leg model. Since the leg model we used was made of rigid plastic, it was relatively easy to hold the hooks in the same locations during actuation. However, slip prevention mechanisms should be more carefully designed and included with real human users in the future.

In addition to the angular displacements, the output forces for active extension and flexion were characterized. Using the same load cell used in the individual muscle characterization test, the force potential of the stationary leg was measured

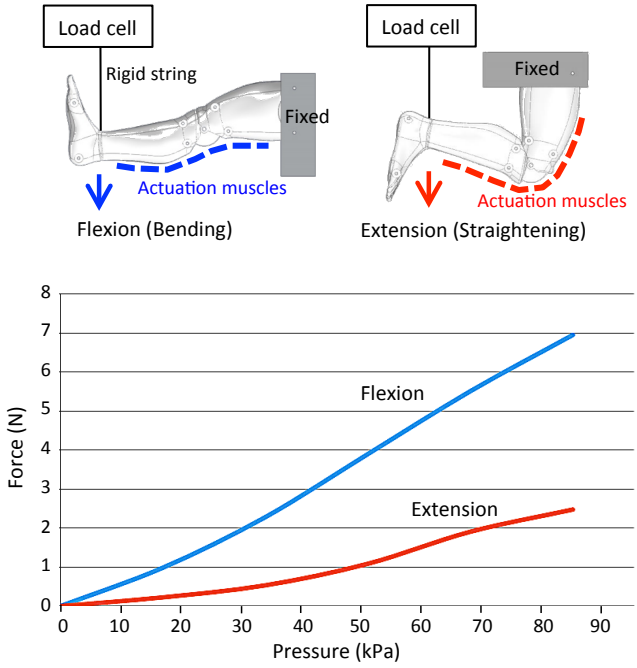

Fig. 11. Knee bending force characterization test setup and result.

at the ankle with the lower leg fixed in the fully flexed and extended orientation as the actuator pressure varied. Fig. 11 shows the result. This test was performed with the force of the device pointed downward, and the initial force applied to the load cell due to the tension of the test setup and the weight of the leg was subtracted from the results. The result shows that the active flexion generates much higher force than the active extension. This is due to the fact that the flexion muscle is located farther away from the axis of rotation than the extension muscle is. The maximum forces measured in this test were approximately 2.5N and 7N for active leg extension and flexion, respectively.

IV. CHALLENGES

There are multiple challenges that must be addressed before we are able to conduct tests with human subjects wearing our Second Skin device.

First, the current prototype is not equipped with any sensing elements. Different types of sensors will be necessary not only for implementing any control algorithms but also for making the device more autonomous and interactive in response to external stimuli. Recent developments of soft sensors can be implemented to detect either external stimuli, such as strain [19], pressure[20], [21], shear stresses [22] or the shape changes of the device, as previously proposed in [7], [23]. Soft sensors can be also directly integrated with artificial muscles to detect their actuation in real-time, as demonstrated in [9], [24]. This type of sensor integrated actuators will provide an active sensing capability to the device for more accurate control without changing its volume and weight.

Second, unlike traditional exoskeletons, the force transmission of the device is realized thorough skin contact. Therefore, the device must be made with non-slippery materials to ensure that sufficient force is transmitted to the wearer. At the same time, the material must allow breathability of skin and must not cause any skin troubles. Use of polymer composites [25], [26] or nano hair structures [27] may be a potential solution to this challenge. Also, a force distribution mechanism should be added to the sleeves to reduce high pressure concentrations around the anchor (hook) locations during actuation.

Another challenge is user safety of the device. Even though the actuators are made of soft materials, they still have the potential to generate high force that could potentially damage the wearer's skin or muscle depending on the input air source. Therefore, a fault detection mechanism must be accompanied when the device is used with human subjects, as discussed in [28], [29]. Also, any failure of an individual actuator must be detected and compensated by the control algorithm to prevent the device from acting in an unexpected or unwanted manner.

V. CONCLUSIONS

A soft wearable robotic device was proposed using compact and lightweight pneumatic artificial muscles. The prototype has eight muscles for bidirectional active knee motions. Each muscle contains four muscle cells creating maximum force of 38N and contraction of 18mm. With different combinations of actuations, the device was able to create active motions for knee extension and flexion. The device was characterized using a 3D printed leg model and demonstrated the maximum knee extension angle of 95° and flexion angle of 37°. The device was also able to generate rotational forces at the ankle approximately 2.5N and 7N for extension and flexion, respectively.

ACKNOWLEDGMENT

The authors would like to thank James Niemi for his support and feedback in this research. We also thank Dr. Diana Young for her suggestions and inputs to this project.

REFERENCES

[1] R. Bogue, "Exoskeletons and robotic prosthetics: a review of recent developments," *Ind. Rob.: Int. J.*, vol. 36, no. 5, pp. 421–427, 2009.

[2] A. B. Zoss, H. Kazerooni, and A. Chu, "Biomechanical design of the Berkeley lower extremity exoskeleton," *IEEE/ASME Trans. Mechatron.*, vol. 11, no. 2, pp. 128–138, 2006.

[3] E. Guizzo and H. Goldstein, "The rise of the body bots," *IEEE Spectrum*, vol. 42, no. 10, pp. 50–56, 2005.

[4] D. P. Ferris, J. M. Czerniecki, and B. Hannaford, "An ankle-foot orthosis powered by artificial peumatic muscles," *J. Appl. Biomech.*, vol. 21, pp. 189–197, 2005.

[5] H. M. Herr and R. D. Kornbluh, "New horizons for orthotic and prosthetic technology: artificial muscle for ambulation," *Proc. SPIE*, vol. 5385, pp. 1–9, 2004.

[6] J. F. Veneman, R. Krudhof, E. E. G. Hekman, R. Ekkelenkamp, E. H. F. V. Asseldonk, and H. van der Kooij, "Design and evaluation of the LOPES exoskeleton robot for interactive gait rehabilitation," *IEEE Trans. Neural Syst. Rehabil. Eng.*, vol. 15, no. 3, pp. 379–386, 2007.

[7] Y.-L. Park, B. Chen, N. O. Pérez-Arancibia, D. Young, L. Stirling, R. J. Wood, E. Goldfield, and R. Nagpal, "Design and control of a bio-inspired soft wearable robotic device for ankle-foot rehabilitation," *Bioinspiration & Biomimetics*, vol. 9, no. 1, p. 016007, 2014.

[8] M. Wehner, Y.-L. Park, C. J. Walsh, R. Nagpal, R. J. Wood, T. Moore, and E. Goldfield, "Experimental characterization of components for active soft orthotics," in *Proc. IEEE Int. Conf. Biomed. Rob. Biomechatron.*, Roma, Italy, June 2012, pp. 1586–1592.

[9] Y.-L. Park, B. Chen, C. Majidi, R. J. Wood, R. Nagpal, and E. Goldfield, "Active modular elastomer sleeve for soft wearable assistance robots," in *Proc. IEEE/RSJ Int. Conf. Intell. Rob. Syst.*, Vilamoura, Portugal, October 2012, pp. 1595–1602.

[10] L. Stirling, C. Yu, J. Miller, R. J. Wood, E. Goldfield, and R. Nagpal, "Applicability of shape memory alloy wire for an active, soft orthotic," *J. Mater. Eng. Perform.*, vol. 20, no. 4-5, pp. 658–662, 2011.

[11] M. Wehner, B. Quindan, P. Aubin, E. Martinez-Villalpando, M. Baumann, L. Stirling, K. Holt, and R. Wood, "A lightweight soft exosuit for gait assistance," in *Proc. IEEE Int. Conf. Rob. Autom.*, Karlsruhe, Germany, May 2013, pp. 3347–3354.

[12] I. Galiana, F. L. Hammond, R. D. Howe, and M. B. Popovic, "Wearable soft robotic device for post-stroke shoulder rehabilitation: Identifying misalignments," in *Proc. IEEE/RSJ Int. Conf. Intell. Rob. Syst.*, Vilamoura, Portugal, October 2012, pp. 317–322.

[13] J. Ueda, D. Ming, V. Krishnamoorthy, M. Shinohara, and T. Ogasawara, "Individual muscle control using an exoskeleton robot for muscle function testing," *IEEE Trans. Neural Syst. Rehabil. Eng.*, vol. 18, no. 4, pp. 399–350, 2010.

[14] C.-P. Chou and B. Hannaford, "Measurement and modeling of McKibben pneumatic artificial muscles," *IEEE Trans. Rob. Autom.*, vol. 12, no. 1, pp. 90–102, February 1996.

[15] N. Saga, T. Nakamura, and K. Yaegshi, "Mathematical model of pneumatic artificial muscle reinforced by straight fibers," *J. Intell. Mater. Syst. Struct.Mater. Sci.*, vol. 18, no. 2, pp. 175–180, 2007.

[16] F. Daerden and D. Lefeber, "The concept and design of pleated pneumatic artificial muscles," *Int. J. Fluid Power*, vol. 2, no. 3, pp. 41–50, 2001.

[17] K. Schneider and R. F. Zernicke, "Mass, center of mass, and moment of intertia estimates for infant limb segments," *J. Biomech.*, vol. 25, no. 2, pp. 145–148, 1992.

[18] H. Sun and R. Jensen, "Body segment growth during infancy," *J. Biomech.*, vol. 27, no. 3, pp. 265–275, 1994.

[19] Y.-L. Park, B. Chen, and R. J. Wood, "Design and fabrication of soft artificial skin using embedded microchannels and liquid conductors," *IEEE Sens. J.*, vol. 12, no. 8, pp. 2711–2718, 2012.

[20] Y.-L. Park, C. Majidi, R. Kramer, P. Berard, and R. J. Wood, "Hyperelastic pressure sensing with a liquid-embedded elastomer," *J. Micromech. Microeng.*, vol. 20, no. 12, p. 125029, 2010.

[21] Y.-L. Park, D. Tepayotl-Ramirez, R. J. Wood, and C. Majidi, "Influence of cross-sectional geometry on the sensitivity of liquid-phase electronic pressure sensors," *Appl. Phys. Lett.*, vol. 101, no. 19, 2012.

[22] D. Vogt, Y.-L. Park, and R. J. Wood, "Design and characterization of a soft multi-axis force sensor using embedded microfluidic channels," *IEEE Sens. J.*, vol. 13, no. 10, pp. 4056–4064, 2013.

[23] Y. Menguc, Y.-L. Park, E. Martinez-Villalpando, P. Aubin, M. Zisook, L. Stirling, R. J. Wood, and C. Walsh, "Soft wearable motion sensing suit for lower limb biomechanics measurements," in *Proc. IEEE/RSJ Int. Conf. Intell. Rob. Syst.*, Karlsruhe, Germany, May 2013, pp. 5289–5296.

[24] Y.-L. Park and R. J. Wood, "Smart pneumatic artificial muscle actuator with embedded microfluidic sensing," in *Proc. IEEE Sens. Conf.*, Baltimore, MD, November 2013, pp. 689–692.

[25] D. D. Rossi, F. Carpi, and E. P. Scilingo, "Polymer based interfaces as bioinspired 'smart skins'," *Adv. Colloid Interfac.*, vol. 116, no. 1-3, pp. 165–178, 2005.

[26] S. Ramakrishna, J. Mayer, E. Wintermantel, and K. W. Leong, "Biomedical applications of polymer-composite materials: a review," *Compos. Sci. Technol.*, vol. 61, no. 9, pp. 1189–1224, 2001.

[27] L. Ge, L. Ci, A. Goyal, R. Shi, L. Mahadevan, P. M. Ajayan, and A. Dhinojwala, "Cooperative adhesion and friction of compliant nanohairs," *Nano Lett.*, vol. 10, no. 11, pp. 4509–4513, 2010.

[28] A. D. Santis, B. Siciliano, A. D. Luca, and A. Bicchi, "An atlas of physical human-robot interaction," *Mech. Mach. Theory*, vol. 43, no. 3, pp. 253–270, 2008.

[29] Y.-L. Park, D. Young, B. Chen, R. J. Wood, R. Nagpal, and E. C. Goldfield, "Networked bio-inspired modules for sensorimotor control of wearable cyberphysical devices," in *Proc. Int. Conf. Comput. Network. Commun. (ICNC)*, San Diego, CA, January 2013, pp. 92–96.